J. Plasma Physics (2006), *vol.* 72, *part* 6, *pp.* 1277–1280. © 2006 Cambridge University Press
doi:10.1017/S002237780600554X Printed in the United Kingdom

Subfemtosecond electron bunch generation by a tightly focused laser pulse

S. MASUDA,[1] K. NAKAJIMA,[2] M. KANDO,[3]
H. KOTAKI,[3] K. KOYAMA,[4] E. MIURA,[4] S. KATO,[4]
M. ADACHI[5] and T. WATANABE[6]

[1]National Institute of Radiological Sciences (NIRS), 4-9-1 Anagawa, Inage, Chiba, Chiba 263-8555, Japan

[2]High Energy Accelerator Research Organization (KEK), 1-1 Oho, Tsukuba, Ibaraki 305-0801, Japan

[3]Japan Atomic Energy Research Institute, 8-1 Umemi-dai, Kizu, Kyoto 619-0215, Japan

[4]National Institute of Advanced Industrial Science and Technology (AIST), Tsukuba Central 2, 1-1-1 Umezono, Tsukuba, Ibaraki 305-8568, Japan

[5]Hiroshima University, 1-3-1 Kagamiyama, Higashi-Hiroshima, Hiroshima 739-8577, Japan

[6]Utsunomiya University, 7-1-2 Yoto, Utsunomiya, Tochigi 321-8585, Japan

(Received 15 August 2005 and accepted 14 February 2006)

Abstract. Three-dimensional electron motion in a linearly polarized tightly focused laser field is numerically calculated. A high-intensity laser pulse focused on the free electrons in vacuum generates relativistic electron bunches whose length is shorter than the laser wavelength. The extremely short electron bunches with low-energy spread less than 1% are generated for a wide range of the laser parameters.

1. Introduction

When a high-intensity laser beam is focused on free electrons in vacuum, the electrons oscillate in the laser polarization direction and are pushed in the laser propagation direction by a Lorentz force. As a result, the electrons are accelerated in the laser propagation direction. Studies on electron acceleration in vacuum by a relativistic laser ponderomotive force have made great progress in recent years, both theoretically [1–10] and experimentally [11–16]. This scheme can generate high-quality electron bunches [7, 9, 10]. In this paper, the length of the electron bunches generated by the laser ponderomotive acceleration in vacuum are estimated numerically. The simulation model is explained in the next section. Section 3 discusses and concludes our simulation results.

2. Simulation model

The electron motion in vacuum is given by the Lorentz force equation, $d(\gamma\beta)/dt = -(e/mc)(\mathbf{E} + \beta \times \mathbf{B})$, where c is the speed of light in vacuum, e is the elementary charge, m is the electron mass, β is the electron velocity normalized by c, $\gamma = 1/\sqrt{1-\beta^2}$ is the normalized energy of the electron, and $\mathbf{E}$ and $\mathbf{B}$ are the electric

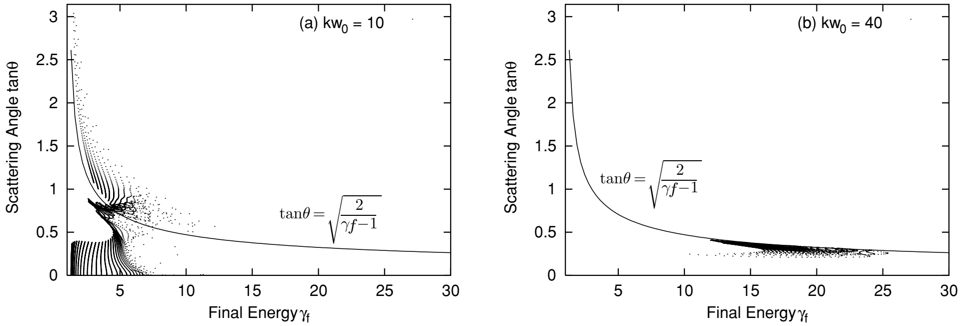

Figure 1. The electron scattering angle as a function of the electron final energy for (a) $kw_0 = 10$ and (b) $kw_0 = 40$.

and magnetic field vector, respectively. The equation is numerically integrated using Boris's algorithm. The transverse electric field of the laser linearly polarized in the x-direction and propagating in the z-direction is given by the paraxial approximation;

$$E_x = E_0(w_0/w)\exp\left[-(x^2+y^2)/w^2\right]\exp(i\Psi)\tau(z,t), \tag{2.1}$$

where the phase is given by $\Psi = \omega t - kz - k(x^2+y^2)/2R + \tan^{-1}(z/z_{\mathrm{R}})$. E_0 is the peak amplitude of the transverse electric field, k is the wave number, $\omega = ck$ is the laser frequency, $w = w_0\sqrt{1+z^2/z_{\mathrm{R}}^2}$ is the laser spot size, w_0 is the spot size at the focus, $z_{\mathrm{R}} = kw_0^2/2$ is the Rayleigh length, and $R = z(1+z_{\mathrm{R}}^2/z^2)$. Here, $\tau(z,t)$ is the laser pulse shape function defined by $\tau(z,t) = \exp[-(t-z/c)^2/4\tau_{\mathrm{L}}^2]$, where τ_{L} is the pulse length. The laser pulse propagates along the z-axis with a velocity c. The center of the pulse reaches the focal point ($z = 0$) at time $t = 0$. The transverse magnetic field is approximated by $B_y = E_x$. When the laser beam is tightly focused to a small spot size comparable to the laser wavelength, the longitudinal components of the laser field cannot be negligible [3, 4]. In the vacuum condition, both divergences of **E** and **B** are zero. The longitudinal components are approximated by [4]

$$\begin{aligned} E_z &= -(i/k)\partial E_x/\partial x \\ &= E_0(w_0/w)\left(i2x/kw^2 - x/R\right)\exp\left[-(x^2+y^2)/w^2\right]\exp(i\Psi)\tau(z,t), \quad (2.2)\\ B_z &= -(i/k)\partial B_y/\partial y \\ &= E_0(w_0/w)\left(i2y/kw^2 - y/R\right)\exp\left[-(x^2+y^2)/w^2\right]\exp(i\Psi)\tau(z,t). \quad (2.3) \end{aligned}$$

3. Results and discussion

In our simulations, the electrons are initially located around the laser focal point. The initial electron energy is set at $\gamma_0 = 1$. The laser pulse with the pulse length of $\omega\tau_{\mathrm{L}} = 20$ is focused on the electrons. The electron scattering angles after the interaction with the laser pulse are plotted in Fig. 1 as a function of the final electron energy for the laser intensity $a_0 = 10$. When the longitudinal components of the laser field are ignored, a quantity $\gamma(1-\beta_z)$ is conserved. In this case, a relation between the scattering angle of the electrons and the electron energy is $\tan\theta = \sqrt{2/(\gamma_f - 1)}$ [1] as shown by a solid curve in Fig. 1. For a large laser spot size ($w_0 = 40$), the scattered electrons distribute around the solid curve due to the small

https://doi.org/10.1017/S002237780600554X Published online by Cambridge University Press

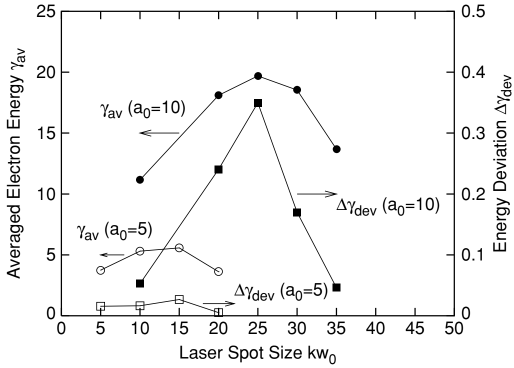

Figure 2. The averaged electron energy and energy deviation as a function of the laser spot size.

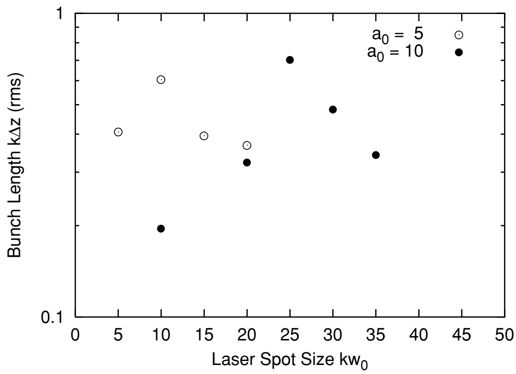

Figure 3. The electron bunch length as a function of the laser spot size.

longitudinal laser field. For a small spot size, the longitudinal components become large and the angle–energy relation is violated. As a result, the transverse electron scattering is suppressed and the number of electrons are scattered in the straight-forward direction as shown in Fig. 1(a). A short bunch is composed at the leading front of the scattered electrons on the z-axis. The averaged energy of the electrons within the bunch is shown in Fig. 2 as a function of the laser spot size. Maximum energy gain is obtained at $kw_0 = 15$ and $kw_0 = 25$ for the laser intensity at $a_0 = 5$ and $a_0 = 10$, respectively. The optimum interaction length to generate the relativistic electron bunch is proportional to a_0^2 [7] as seen from Fig. 2. For shorter or longer interaction lengths far from the optimum condition, the energy gain is small and a clear electron bunch is not produced. The energy deviation of the electrons in the bunch is also shown in Fig. 2. The deviation has maximum value at the optimum interaction length. The energy spread $\Delta\gamma_{\text{dev}}/\gamma_{\text{av}}$ is less than 1% for $a_0 = 5$ and does not exceed 2 % for $a_0 = 10$.

Figure 3 shows the bunch length of the electrons as a function of the laser spot size w_0 for both $a_0 = 5$ and $a_0 = 10$. The spot size w_0 with respect to the maximum bunch length is obtained near the optimum w_0 for the maximum energy gain. In our simulations, the bunch length does not exceed $1/k$, that is 130 nm for a $\lambda = 800$ nm laser, independent of the laser intensity. The high-quality monoenergetic subfemtosecond electron bunches are produced in the range of kw_0 from 5 to 20 at $a_0 = 5$ and from 10 to 35 for $a_0 = 10$. It can be seen from Figs 2 and 3 that the normalized longitudinal emittance

$$\epsilon_{zn} = \sqrt{\langle (z - \langle z \rangle)^2 \rangle \langle (\gamma\beta_z - \langle \gamma\beta_z \rangle)^2 \rangle - \langle (z - \langle z \rangle)(\gamma\beta_z - \langle \gamma\beta_z \rangle) \rangle^2} \approx \Delta z \Delta\gamma_{\mathrm{dev}},$$

is less than $1/k$ in the range of the simulated parameters.

References

[1] Hartemann, F. V., Foches, S. N., LeSage, G. P., Luhmann, N. C., Woodworth, J. G., Pery, M. D. and Chen, Y. J. 1995 Nonlinear ponderomotive scattering of relativistic electrons by an intense lasesr field at focus. *Phys. Rev. E* **51**, 4833–4843.

[2] Esarey, E., Sprangle, P. and Krall, J. 1995 Laser acceleration of electrons in vacuum. *Phys. Rev. E* **52**, 5443–5453.

[3] Hartemann, F. V., Van Meter, J. R., Troha, A. L., Landahl, E. C., Luhmann, N. C., Baldis, H. A., Gupta, A. and Kerman, A. K. 1998 Three-dimensional relativistic electron scattering in an ultrahigh-intensity laser focus. *Phys. Rev. E* **58**, 5001–5012.

[4] Quesnel, B. and Mora, P. 1998 Theory and simulation of the interaction of ultraintense laser pulses with electron in vacuum. *Phys. Rev. E* **58**, 3719–3732.

[5] Troha, A. L., Van Meter, J. R., Landahl, E. C., Alvis, R. M., Unterberg, Z. A., Li, K., Luhmann, N. C., Kerman, A. K. and Hartemann, F. V. 1998 Vacuum electron acceleration by coherent dipole radiation. *Phys. Rev. E* **60**, 926–934.

[6] Kong, Q., Ho. Y. K., Wang, J. X., Wang, P. X., Feng, L. and Yuan, Z. S. 2000 Conditions for electron capture by an ultraintense stationary laser beam. *Phys. Rev. E* **61**, 1981–1984.

[7] Stupakov, G. V. and Zolotorev, M. S. 2001 Ponderomotive laser acceleration and focusing in vacuum for generation of attosecond electron bunches. *Phys. Rev. Lett.* **86**, 5274–5277.

[8] Hartemann, F. V. 2002 In: *High-Field Electrodynamics*. Boca Raton, FL: CRC Press.

[9] Kong, Q., Miyazaki, S, Kawata, S., Miyauchi, K., Nakajima, K., Masuda, S., Miyanaga, N. and Ho, Y. K. 2003 Electron bunch acceleration and trapping by the ponderomotive force of an intense short-pulse laser. *Phys. Plasmas* **10**, 4605–4608.

[10] Masuda, S., Kando, M., Kotaki, H. and Nakajima, K. 2005 Suppression of electron scattering by the longitudinal components of tightly focused laser fields. *Phys. Plasmas* **12**, 013102.

[11] Malka, G. and Miquel, J. L. 1996 Experimental confirmation of ponderomotive-force electrons produced by an ultrarelativistic laser pulse on solid target. *Phys. Rev. Lett.* **77**, 75–78.

[12] Malka, G., Lefebvre, E. and Miquel, J. L. 1997 Experimental observation of electrons accelerated in vacuum to relativistic energies by a high-intensity laser. *Phys. Rev. Lett.* **78**, 3314–3317.

[13] Moore, C. I., Ting, A., McNaught, S. J., Qiu, J., Burris, H. R. and Sprangle, P. 1999 A laser-accelerator injector based on laser ionization and ponderomotive acceleration of electrons. *Phys. Rev. Lett.* **82**, 1688–1691.

[14] Chaloupka, J. L. and Meyerhofer, D. D. 1999 Observation of electron trapping in an intense laser beam. *Phys. Rev. Lett.* **83**, 4538–4541.

[15] Moore, C. I., Ting, A., Jones, T., Briscoe, E., Hafizi, B., Hubbard, R. F. and Sprangle, P. 2001 Measurements of energetic electrons from the high-intensity laser ionization of gases. *Phys. Plasmas* **8**, 2481–2487.

[16] Ting, A., Kaganovich, D., Gordon, D. F., Hubbard, R. F. and Sprangle, P. 2005 Generation and measurements of high energy injection electrons from the high intensity laser ionization and ponderomotive acceleration. *Phys. Plasmas* **12**, 010701.